Post-transcriptional Regulation of *Lfng* by miR-125a is Crucial for Vertebrate Segmentation

Maurisa F. Riley[1]

1. Department of Molecular Genetics, The Ohio State University, Columbus, OH 43210

Corresponding Author riley.295@osu.edu

Abstract

Somites are the embryonic precursors of vertebrae, ribs, and skeletal muscles. They form from the presomitic mesoderm (PSM) by a periodic segmentation process called somitogenesis. The periodic budding of somites is controlled in part by the oscillatory expression of genes such as Lunatic fringe (*Lfng*), a modulator of Notch signaling, which function in a segmentation clock that times somitogenesis. Proper clock function requires that both the mRNA half-lives of oscillatory genes and the translational efficiency of these transcripts be tightly controlled during the rapid time period of the clock. We propose that microRNAs (miRs) have a conserved function in the segmentation clock through post-transcriptional regulation of oscillatory genes. We demonstrate that *Lfng* is a conserved target of two miRs (miR-125a-5p and miR-200b) enriched in the PSM, where the segmentation clock is active. Blocking interactions between one of these miRs (miR-125a-5p) and *Lfng* in developing chick embryos abolishes oscillatory gene expression of endogenous *Lfng* and *cHairy1*, resulting in disrupted somite formation and patterning. These findings suggest that miR:transcript interactions may modulate the oscillatory expression of clock-linked genes by affecting mRNA turnover and/or translational efficiency. The data presented in this paper provide the first evidence supporting a role for miRs in the segmentation clock and enhance our understanding of post-transcriptional regulation of oscillatory genes.

Introduction

Vertebrate somitogenesis is the process by which somites give rise to the axial skeleton, the dermis of the back, and skeletal muscle (Hirsinger E 2000). These highly organized blocks of epithelial tissue are comprised of cohorts of cells that bud from the anterior end of the presomitic mesoderm (PSM). This highly regulated event is controlled in part by a molecular oscillator named the segmentation clock. Linked to this clock is expression of oscillatory genes, such as Lunatic fringe (*Lfng*), that function to time the periodic budding of somites. *Lfng* encodes a glycosyltransferase that modifies the Notch receptor in the Golgi complex to modulate Notch signaling (Hicks C 2000). During vertebrate segmentation, *Lfng* transcript and LFNG protein levels oscillate with a period that matches somite formation (two hours in mouse; 90 min in chick), connecting both mRNA and protein expression levels to the segmentation clock (Forsberg H 1998; McGrew MJ 1998; Dale JK 2003).

Lfng is required for both somite segmentation and rostral-caudal patterning. Complete loss of *Lfng* in mice results in severe skeletal abnormalities demonstrated by truncated tails and shortened body axes. Lunatic fringe mutant embryos have defects in somite segmentation and rostral-caudal somite patterning (Evrard YA 1998; Zhang Gridley 1998). Interestingly, constitutive expression of *Lfng* in mice (Serth K 2003) and overexpression of *Lfng* in chick (Dale JK 2003) result in similar somite and skeletal phenotypes. These results demonstrate that loss of *Lfng* or sustained *Lfng* activity have similar effects on somite formation and patterning, presumably by perturbing the oscillatory nature of the endogenous expression. These results indicate that tight control of *Lfng* mRNA and protein are essential for proper segmentation clock function.

Although it is known that cyclic *Lfng* expression is regulated at the transcriptional level (Cole SE 2002; Morales AV 2002), little is known about the post-transcriptional mechanisms that contribute to the rapid oscillations. *Lfng* has been proposed to function in a negative feedback loop with *Notch* and *Hes7*. In mathematical models of this oscillator, the mRNA and protein half-lives of *Lfng* and *Hes7* must be tightly regulated to ensure proper segmentation clock function (Xie ZR 2007). Indeed, post-transcriptional regulation of Hes7, which exhibits the same dynamic expression pattern as *Lfng* in the PSM, is essential for the segmentation clock. Mice expressing a mutant form of Hes7, where the half-life is lengthened from ~22 min to ~30 minutes, have disrupted somite segmentation and exhibit noncyclical expression of Hes7 mRNA and protein in the PSM (Hirata H 2004). Our lab (unpublished) and others (Chen J 2005; Hilgers V 2005) have demonstrated that the *Lfng* 3'UTR is important for controlling *Lfng* mRNA stability. Given that the *Lfng* 3'UTR is evolutionarily conserved, it is plausible that regulatory sequences within this region facilitate the rapid oscillations necessary for proper segmentation and clock function.

Post-transcriptional regulation via untranslated regions is a well-established concept (Wightman B 1993; Levy AP 1996; Lai EC 1997; Tadauchi T 2001; Xie X 2005). It is widely accepted that oscillatory expression of genes such as *Lfng* and *Hes7* results from a delayed negative feedback loop where the proteins repress the transcription of their own genes via regulatory sequences in the 5' regulatory regions. Various groups have supported this theory through mathematical modeling based upon oscillatory dynamics observed *in vivo* (Baker RE 2008). The mathematical modeling of the negative feedback loops relies on the basic fact that neither transcription nor translation is an instantaneous process. In a negative feedback loop, there is a time lag between the start of transcription and the auto-repressive action of the protein

product. This time delay allows for the transcription rate of the coding gene to increase to a certain threshold before the protein product can repress transcription. Once the concentration of protein surpasses this threshold, the rate of gene transcription will decrease, resulting in decreased protein, which in turn causes the rate of transcription to increase again.(Lewis 2003; Monk 2003; Hirata H 2004; Zeiser S 2006; Xie ZR 2007). Hence, a delayed negative feedback loop can give rise to the oscillatory gene expression exhibited by *Lfng*.

A recent model of oscillatory gene expression with delayed negative feedback includes an additional component: microRNA (miRNA) regulation of both mRNA degradation and translational repression. miRNAs have been shown to regulate a wide variety of biological processes including cell proliferation, apoptosis, neurogenesis, and cardiogenesis (Ambros 2004; Bartel 2004). miRNAs are non-coding RNA molecules of ~21 nucleotides in length that direct post-transcriptional repression of protein-coding genes. They make up 1-3% of the genome and are generated by a multi-step process that results in their association with a protein complex known as the RNA-induced silencing complex (RISC). RISC can bind to mRNA transcripts and target them to P-bodies for degradation or sequestration from translation. Target recognition is primarily based upon pairing between nucleotides 2-7 in the 5' region of the miRNA and the 3'UTR of the target mRNA. In the context of the delayed negative feedback loop, miRNAs can influence mRNA stability and/or translational time lag to regulate oscillatory gene expression.

A recent mathematical model incorporating miRNA regulation predicts that cyclic expression dynamics can only be observed when the mRNA half-life and protein output are limited to a narrow range (Xie ZR 2007). Based upon this model, slight changes in mRNA stability and/or translational repression can result in stable expression dynamics. As previsouly mentioned, both loss of expression and constitutive, non-cyclic expression of *Lfng* have a similar

detrimental impact on somite formation and patterning, demonstrating the importance for tight regulation of *Lfng* expression (Evrard YA 1998; Zhang Gridley 1998; Dale JK 2003; Serth K 2003; Shifley ET 2008). We hypothesize that oscillatory expression of *Lfng* requires post-transcriptional regulation mediated by miRNAs in order to fine-tune the specific timing requirements for expression during somitogenesis. Consistent with the fact that *Lfng* oscillations are essential for proper avian (Dale JK 2003) and murine (Serth K 2003; Shifley ET 2008) somite segmentation and patterning, we demonstrate that blocking *Lfng*-microRNA interactions perturbs cyclic expression of endogenous *Lfng* resulting in disrupted somite formation and rostral-caudal patterning.

RESULTS

Specific expression of miR-200 and 125a-5p in murine presomitic mesoderm

A molecular clock that regulates vertebrate segmentation drives the cyclic expression of *Lfng* in the PSM. The *Lfng* mRNA half-life and protein output must be tightly controlled in order to maintain oscillatory expression and proper clock function. We hypothesize that if microRNAs facilitate this regulation, a subset of them will be enriched in the PSM where the clock is active. Two web-based target prediction algorithms, TargetScan (Lewis BP 2003) and miRanda (John B 2004), indicate that *Lfng* is a potential target of miR-200bc/429, miR-125a-5p/125b-5p/351, and miR-204/211 (Fig. 1A). In order to determine whether any of these microRNAs are enriched in the PSM, we performed TaqMan MicroRNA assays to quantify these mature microRNAs in tissue derived from the PSM and mature somites of E9.5 mouse embryos. Of the 8 microRNAs examined, 3 were significantly upregulated, 2 were significantly down regulated, and 3 were unchanged in the PSM (Fig. 1B). To examine the potential role of miR:transcript interactions in the clock, we focused on miRs upregulated in the PSM. We then verified the expression of a subset of these microRNAs (mmu-miR-200b and mmu-miR-125a-5p) via whole mount in situ hybridization with locked nucleic acids (LNAs) antisense to mmu-miR-200b and mmu-miR-125a-5p. Consistent with the RT-PCR results, both microRNAs were specifically expressed in the caudal PSM and reduced or absent in the mature somites (Figure 1C-D). These results demonstrate that 2 miRs (mmu-miR-125a-5p and mmu-miR-200b) predicted to target *Lfng* are enriched in the PSM where the segmentation clock is active.

Lfng is a target of miR-125a-5p and miR-200b

Given the specific expression of mmu-miR-200b and mmu-miR-125a-5p in the PSM, where *Lfng* exhibits oscillatory expression dynamics, we tested whether the mouse *Lfng (*m*Lfng)*

3’-UTR is a target for either of these miRs. *Lfng* has one highly conserved putative microRNA binding site for miR-200b (7-base-pair match in seed region at position 645-651) (Fig. 1A) and one for miR-125a-5p (8 –base-pair match in seed region at position 993-999) (Fig. 1A) in the mouse 3’UTR. There are also two putative less-conserved binding sites for miR-125a-5p (positions 186-192 and 297-303), one of which is also found in other mammalian transcripts (Fig. 1A). The mouse *Lfng* (m*Lfng*) 3’-UTR was cloned downstream from a luciferase reporter gene and transfected into 3T3 cells. Inclusion of the *Lfng* 3’UTR results in a 34% reduction in luciferase expression levels compared to control, presumably due to activity of endogenous miRs (Fig. 2C). When premiR-200b is co-transfected with constructs containing the *Lfng* 3’UTR, luciferase levels are reduced by 51% compared to co-transfection of this construct with scrambled premiR. Mutation of the predicted miR-200b binding site abrogates this effect, indicating that miR-200b can directly target the m*Lfng* 3’UTR (Fig. 2A). Similarly, co-transfection of premiR-125a-5p reduces luciferase activity by 72% for this construct, and mutations in either the conserved or both non-conserved binding sites abrogate this effect. This may indicate that there is cooperation between the miR-125a sites in the m*Lfng* 3’UTR to regulate expression of the reporter gene (Fig. 2B). Co-transfection of both premiR-200b and premiR-125a-5p does not significantly affect the reduction in luciferase activity compared to single transfections. However, when a luciferase construct bearing the m*Lfng* 3’UTR with mutations in all four binding sites for miR-200b and 125a-5p is introduced into 3T3 cells, we observe that the 34% reduction in luciferase levels observed after co-transfection with Lfng 3’UTR and scrambled premiR is lost (Fig. 2C) This supports the hypothesis that binding of endogenous miRs to the m*Lfng* 3’-UTR is responsible for the 34% reduction in luciferase protein levels in 3T3 cells in the absence of exogenous miRs .

One of the binding sites for miR-125a-5p and the binding site for miR-200b in the *Lfng* 3'UTR are evolutionarily conserved among mouse, human, and chicken (Fig. 1A). To examine the evolutionary conservation of this relationship, we cloned the chick *Lfng* 3'UTR (*cLfng*) downstream of a luciferase reporter to determine whether it is also a bona fide target of these miRs. Luciferase levels for this construct are reduced 85% in the presence of premiR-125a-5p and reduced 70% in the presence of premiR-200b. Mutations in the binding sites for these miRs abrogate this effect, indicating that the c*Lfng* 3'UTR is a specific target for miR-200b and 125a-5p in 3T3 cells (Fig. 2D). Together, these results support the idea that the *Lfng* 3'UTR is an evolutionarily conserved target of two miRs enriched in the PSM, supporting the hypothesis that miRs may have a conserved function in the segmentation clock by binding to the 3'UTRs of oscillatory genes and fine-tuning mRNA stability and/or translational efficiency.

Blocking miR-125a/*Lfng* interactions disrupts somite formation and patterning in chick embryos

The segmentation clock operates in a similar manner during mouse and chicken somitogenesis (Gomez C 2008). To examine the *in vivo* roles of miR-200b:*Lfng* and miR-125a:*Lfng* interactions during vertebrate segmentation, we utilized Target Protectors (TP) (Choi WY 2007) to specifically disrupt the interaction of endogenous miRNAs with endogenous *Lfng* transcripts in developing chick embryos. Target Protectors morpholinos have been successfully used to interfere with miRNA mediated repression of specific 3'UTRs in zebrafish (Choi WY 2007; Leucht C 2008; Zeng L 2009), in cardiomyocytes (Lin Z 2009), and in cell lines (Sheedy FJ 2010). In tissue cultures, these TPs do not themselves affect luciferase activity from constructs containing the chick *Lfng* 3'UTR, but do protect *Lfng* 3'UTR containing transcripts from the effects of exogenously introduced miRNAs (Supplementary Figure 1). Due to the

accessibility of chicken embryos by in ovo electroporation, we utilized TPs to study whether blocking *Lfng*:miR-200b or *Lfng*:miR-125a interactions affect the segmentation in this system. We designed fluorescein-tagged TPs complementary to the regions of the miR-200b (*Lfng*-$TP^{miR\text{-}200}$) and miR-125a (*Lfng*-$TP^{miR\text{-}125a}$) target sites in the *cLfng* 3'-UTR, as well as a control TP complementary to a unique random site in the *cLfng* 3'UTR (*Lfng*-TP^{ctrl}) (Fig 3A).

To examine the effect of blocking miR-200b:*Lfng* and miR-125a:*Lfng* interactions on segmentation, we introduced these TPs into Hamburger-Hamilton (HH) stage 7-9 (Hamburger and Hamilton 1992) chick PSM via in ovo electroporation (Dubrulle J 2001), and allowed embryos to develop for 24 hours until the electroporated regions had undergone segmentation. Blocking interactions between *Lfng* and both miR-125a and miR-200b significantly perturbed segmentation as evidenced by the formation of abnormally sized somites with irregularly positioned boundaries (n=15; compare Fig. 3C and G). The expression of *Uncx4.1* is normally restricted to the caudal half of the somite (Fig. 3C). In embryos where miR-125a/200:*Lfng* interactions are blocked, the Uncx4.1 expression is normal in the early somites formed from un-electroporated tissues, but is irregular or completely absent in fluorescein positive somites (Fig. 3G). MyoD expression in the myotome compartment indicates that somites arising from *Lfng*-$TP^{miR\text{-}125a+200b}$ electroporated tissues undergo differentiation, but these compartments exhibit abnormal size and spacing, reflecting the underlying defects in somite morphogenesis. (Compare Fig. 3E and I). These data indicate that blocking interactions between *Lfng* and both miR-125a and miR-200b perturbs rostral-caudal somite patterning and somite segmentation, although somite differentiation is unaffected. To dissect the specific roles of these miRs in segmentation, we electroporated embryos with *Lfng*-$TP^{miR\text{-}125a}$ alone and observed a similar phenotype indicating perturbed somite segmentation and patterning (Fig. 3K;M). In contrast,

electroporation of *Lfng*-TP$^{miR\text{-}200b}$ alone (Fig. 3O;Q) or Lfng-TP^{ctrl} (Fig. 3C;E) had no observable effect on segmentation or on expression of these marker genes. These data indicate that interactions between miR-125a and *Lfng* are essential for somite formation and rostral-caudal patterning in the developing chick embryo.

Disrupting miR-125a/*Lfng* interactions perturbs cyclic gene expression in the chick PSM

Lfng oscillations are essential for proper avian (Dale JK 2003) and murine (Serth K 2003; Shifley ET 2008) somite formation and patterning. In the PSM of mouse and chick embryos, *Lfng* is dynamically expressed in three distinct phases that narrow as it moves anteriorly. During Phase I, *Lfng* is expressed as a broad domain throughout the caudal half of the PSM with a narrow band in the rostral-most part of the PSM. During Phase II, the expression domain narrows towards the middle of the PSM and the rostral band fades in intensity. During Phase III, the expression domain becomes an intense narrow band in the rostral-most compartment of the PSM.

To examine the effect of blocking miR-200b:*Lfng* and miR-125a:*Lfng* interactions on oscillatory genes in the segmentation clock, we introduced these TPs into Hamburger-Hamilton (HH) stage 7-9 (Hamburger and Hamilton 1992) chick PSM via in ovo electroporation (Dubrulle J 2001). Embryos were examined for fluorescein expression in the PSM 8 hours post-electroporation. Fluorescein-positive embryos were used to analyze the expression profile of endogenous *Lfng* mRNA. Of 12 embryos electroporated with *Lfng*-TP^{ctrl}, 4 embryos express *Lfng* in a phase I domain, 4 in a phase II domain, and 4 in a phase III domain (Fig. 4A). This ratio is similar to that observed in non-electroporated embryos (Supplementary Fig. 2A). In contrast, of 12 embryos electroporated with both *Lfng*-TP$^{miR\text{-}200}$ and *Lfng*-TP$^{miR\text{-}125a}$, none exhibit *Lfng* mRNA expression in the caudal PSM. Rather, all 12 embryos express *Lfng* as a smear, expressed

in the rostral-most compartment of the PSM, extending into the middle of the PSM in some embryos (Fig. 4B). In ovo electroporation of *Lfng*-TP$^{miR\text{-}125a}$ alone results in a similar expression pattern of endogenous *Lfng* with only one phase observed in 12 embryos examined and no expression observed in the caudal PSM (Fig. 4C). In contrast, after in ovo electroporation of *Lfng*-TP$^{miR\text{-}200}$ alone, we observe an oscillatory expression pattern of endogenous *Lfng* similar to that seen in control embryos (Fig. 4D). This suggests that interactions between endogenous miR-125a and *Lfng* transcripts are essential for maintaining endogenous *Lfng* oscillations in the PSM.

Since *Lfng* functions in a negative feedback loop with *cHairy1*, we examined the effects of Lfng- TP$^{miR\text{-}200b}$ or *Lfng*-TP$^{miR\text{-}125a}$ on endogenous *cHairy* expression. Similar to *Lfng*, *cHairy1* expression oscillates among three distinct phases in wild type embryos (Supplementary Figure 2B). We find that disrupting interactions between miR-125a/miR-200b and *Lfng* perturbs *cHairy* oscillations, while embryos electroporated with TP-*Lfng*^{Ctrl} exhibit wild type expression (compare Fig. 4 E and F). Similarly, disrupting interactions between miR-125a and *Lfng* results in similar perturbation of endogenous *cHairy1* oscillations (compare Fig. 4E and G). Taken together, these results indicate that interactions between miR-125a and *Lfng* are essential for maintaining cyclic gene expression in the PSM, and disruption of these interactions leads to abnormal somite segmentation and rostral-caudal patterning.

Discussion

Our results demonstrate that microRNAs play a conserved role in the vertebrate segmentation clock through post-transcriptional regulation of *Lfng*. Although work from our lab and others demonstrate that *Lfng* oscillations are regulated at the transcriptional level(Cole SE 2002; Morales AV 2002), little is known about mechanisms of post-transcriptional control that contribute to these rapid oscillations. Unpublished work from our lab using transgenic mice indicates that although the *Lfng* promoter contains the regulatory elements sufficient for transcriptional oscillations in the PSM, the *Lfng* 3'UTR contains elements necessary to sustain these oscillations and regulate *Lfng* stability. The results presented here demonstrate that interactions between miR-125a and the *Lfng* 3'UTR are essential for post-transcriptional regulation of oscillatory genes in the segmentation clock.

miRNA-125a-5p plays a tuning function in the segmentation clock

We propose that miR-125a-5p and *Lfng* exhibit tight co-expression in the PSM in order to facilitate a tuning function for this microRNA in the segmentation clock. Various groups have hypothesized that microRNAs that are specifically co-expressed with their target could function to dampen protein output or adjust mRNA levels to an optimal but still functional level (Xie ZR 2007; Shkumatava A 2009). This function is very different from the more common "fail-safe" function to reduce mRNA and/or protein output to non-functional, inconsequential levels. We find that mmu-miR-125a-5p and its target, *Lfng*, are co-expressed specifically in the PSM, where the segmentation clock is active, compared to mature somites. Blocking interactions between miR-125a and *Lfng* in the developing chick PSM results in perturbed *Lfng* and *cHairy* oscillations, confirming a tuning function for this interaction *in vivo*. If miR-125a has a fail-safe function in the clock, we would expect to observe a significant increase in expression of its target

upon blocking miR-125a:*Lfng* interactions. Rather, we observe an alteration of the oscillatory expression pattern of endogenous *Lfng*, indicating that under normal circumstances, miR-125a functions to optimize *Lfng* expression in order to maintain oscillations during the rapid period of the clock.

miR-mediated post-transcriptional regulation facilitates the oscillation machinery

Lfng is an internal component of the oscillating machinery, functioning in a negative feedback loop to periodically repress *cHairy* (chick homolog of *Hes7*) transcription. As a result, interfering with miR-125a:*Lfng* interactions perturbs oscillations of both *Lfng* and *cHairy* in the PSM. These results are consistent with mathematical models of the segmentation clock, where microRNAs facilitate oscillatory dynamics generated by the delayed negative feedback loop. In this model, microRNAs operate in concert with the other regulatory machinery of the cell to sustain oscillations during the rapid period of the clock.

We find that preventing interactions between miR-125a and *Lfng* results in stable expression dynamics and propose that miR-125a functions to regulate *Lfng* mRNA stability and/or or repress translation. At this time we cannot distinguish between these two possibilities in this system, as *Lfng* functions in a delayed negative feedback loop, and both miR-mediated functions ultimately result in stable mRNA and protein expression dynamics in computer models. Mathematical models of cyclic expression dynamics demonstrate that increasing mRNA half-life by as little as 13 minutes results in dampened oscillations which may be below the threshold of observation (Xie ZR 2007). If miR-125a functions to regulate *Lfng* mRNA stability, this could explain the stable expression of endogenous *Lfng* observed after blocking *Lfng*:miR-125a interactions in the PSM. Extensive analysis of protein and mRNA changes upon loss of specific microRNAs in cell culture reveal that a small group of genes are affected exclusively at

the protein level with little or no change at the mRNA level. However, the targets repressed at the translational level were repressed modestly, consistent with a fine-tuning miR-mediated function, whereas for targets undergoing robust repression, the mechanism of repression was mRNA destabilization (Baek D 2008). Based upon these findings, it is plausible that miR-125a regulates *Lfng* mRNA stability in addition to repressing LFNG protein output in order to fine-tune rather than control the switch between on and off states during the segmentation clock.

Although members of the miR-200 family have been shown to target the *Lfng* 3'UTR in cell culture (Fig. 2) and in zebrafish using GFP reporters (Choi PS 2008), it does not appear to play a role in the chick segmentation clock. miR-200b/c is strongly expressed in the ectoderm of chick embryos (Darnell DK 2006) and functions to mediate such developmental processes as epithelial to mesenchymal transition (Gregory PA 2008; Korpal M 2008) and olfactory neurogenesis (Choi PS 2008). The enrichment of miR-200b/c in the PSM identified by our RTPCR and whole mount in-situ hybridization results could have resulted from the thick ventral ectodermal ridge (VER) present on the ventral surface of the PSM near the tip of the tail. We attribute our observed enrichment of miR-200b/c in the PSM to its expression in the VER and conclude that these microRNAs most likely do not function in the mesoderm of developing chick embryos.

Our results demonstrate that post-transcriptional regulation of *Lfng* by miR-125a is essential for oscillatory expression of *Lfng* in the PSM and for normal somite segmentation and rostral-caudal patterning. Although *Lfng* oscillations in the PSM are essential for proper clock function, *Lfng* has also been implicated in somite boundary formation independent of the segmentation clock. At this point we cannot rule out the possibility that the segmentation defects observed upon blocking miR-125a:*Lfng* interactions may result from a disruption in this process

rather than from a disruption in segmentation clock function. However, recent results suggest that the most important role of *Lfng* during somitogenesis is in the segmentation clock (Oginuma M 2010). Irrespective of this point, our results reveal a novel mechanism of post-transcriptional regulation in the segmentation clock. Since the mRNA half-lives and protein output of other oscillatory genes, such as *Hes7*, must be tightly controlled during the rapid period of the clock, it is possible that miR-mediated regulation could fine-tune these specific timing requirements for other oscillatory genes in the segmentation clock.

Materials and Methods

RTPCR. RNA from PSM and 5 most recently formed somites from 50 mouse E9.5 embryos extracted and used for qRTPCR of 7 microRNAs using Taqman® probes from Applied Biosystems (hsa-miR-200c, 2300, PN4395411; hsa-miR-200b, 2251, PN4395362; hsa-miR-125a-5p, 2198, PN4395309; hsa-miR-125b, 449, PN4373148; mmu-miR-351, 1067, PN4373345; mmu-miR-204, 508, PN4373094; mmu-miR-211, 1199, PN4373315; mmu-miR-429, 1077, PN4373355; snoRNA135, snoRNA234 were used for normalization.

Luciferase Assays. The *Lfng* 3'UTR was amplified from mouse genomic DNA (5'GTCGTGGTTGAAACTCTGTCC and 5'CAGAGGAAGGACGTCACCAT) and chick genomic DNA (5' GCTCTAGATCGTTGCTGTGGTATTGC and 5'CGTCTAGAGCTGCTTTATTGGTGACG) and cloned into the pMIR-REPORT™ Luciferase Reporter vector (Ambion). Mutations in the miR-125a-5p and miR-200b seed regions of the *Lfng* 3'UTR were generated using PCR-based mutagenesis and confirmed by sequencing. Amplified 3'UTRs were cloned downstream of the firefly luciferase coding region in the pMIR-REPORT™ (Ambion). NIH3T3 cells were plated in 24-well plates (4×10^4 cells per well) 24 h prior to co-transfection of 100ng reporter vector, 10ng pSV Renilla as a transfection control, and 30nM of synthetic precursor miRNA (pre-miRs) (Ambion). Cells were collected 40 h after transfection and assayed for luciferase activity using the dual luciferase kit (Promega).

Chicken embryo manipulation. Fertilized chick eggs were incubated at 37°C and staged according to Hamburger and Hamilton(Hamilton 1951). For in ovo electroporation, eggs were developed until stage 7-9, windowed, and injected with Indian ink (1:20) to reveal the embryo. Using a glass capillary, morpholinos (500uM in 5% sucrose containing 50ng/ul pCAAX as 'carrier) were laid on the epiblast of the anterior primitive streak. Immediately, the platinum

electrode (anode) is positioned in the yolk with the tip of the electrode positioned underneath the anterior primitive streak and the tungsten electrode (cathode) is placed on the area to be targeted (anterior primitive streak). A current of 6V (3 pulses, 250ms duration, 975ms interval) was applied across the electrodes. After electroporation, embryos were incubated for 8h or 24h at 38°C. After incubation, embryos were collected and assessed for fluorescein expression. Embryos showing both a normal morphology outside the fluorescein-positive domain and a high intensity of fluorescein in the PSM (8h post-electroporation) or mature somites (24h post-electroporation) were fixed in 4% paraformaldeyhde for 4h at room temperature and analyzed by *in situ* hybridization. A total of 592 embryos were electroporated, and of these, 132 fluorescein positive embryos were analyzed.

***In situ* Hybridization.** RNA in situ hybridization using digoxigenin-labeled probes was performed essentially as described (Riddle RD 1993); however, embryos were blocked in a mixture of MABT +20% sheep serum +2% Boehringer blocking reagent; all post-antibody washes were performed in MABT. The chick UNCX4.1 probe was amplified from chick genomic DNA (5'ccaacaaacccgacaaaaac and 5'ttgtcgcggtacagtttgtc), the *cLfng* coding probe was amplified from chick cDNA (5' gaagcaagcacgaaatgtca and 5' gagaaggctcccttcatgtg), the *cHairy* coding probe was amplified from chick cDNA (5' gacacgggcatggaaaaa and 5'acacgtgcccaaatgatgt), and the cMyoD coding probe was amplified from chick cDNA (5' agctctcgcaggagaaacag and 5' tccgtattcaagagccaggt).

Wholemount in situ hybridization was performed essentially as described (Kloosterman Nature Methods 2006). 5' –DIG labeled miRCURY LNA^{TM} Detection probes (Exiqon) for mmu-miR-125a-5p and mmu-miR-200b were labeled using the DIG 3'-End labeling kit (Roche).

Hybridization was carried out overnight at the following temperatures: 50°C for mmu-miR-200b LNA Detection probe and 52°C for mmu-miR-125a-5p Detection LNA probe.

References

Ambros, V. 2004. The functions of animal microRNAs. *Nature* 431: 350-5.

Baek D, V.J., Shin C, Camargo FD, Gygi SP, Bartel DP. 2008. The impact of microRNAs on protein output. *Nature* 455: 64-71.

Baker RE, S.S., Maini PK. 2008. Mathematical models for somite formation. *Curr Top Dev Biol.* 81: 183-203.

Bartel, D. 2004. MicroRNAs: genomics, biogenesis, mechanism, and function. *Cell* 116: 281-97.

Bray N, D.I., Pachter L. 2003. AVID: A global alignment program. *Genome Res.* 13: 97-102.

Chen J, K.L., Zhang N. 2005. Negative feedback loop formed by Lunatic fringe and Hes7 controls their oscillatory expression during somitogenesis. *Genesis* 43: 196-204.

Choi PS, Z.L., Choi WY, Caron S, Alvarez-Saavedra E, Miska EA, McManus M, Harfe B, Giraldez AJ, Horvitz HR, Schier AF, Dulac C. 2008. Members of the miRNA-200 family regulate olfactory neurogenesis. *Neuron* 57: 41-55.

Choi WY, G.A., Schier AF. 2007. Target protectors reveal dampening and balancing of Nodal agonist and antagonist by miR-430. *Science* 318: 271-4.

Cole SE, L.J., Tilghman SM, Vogt TF. 2002. Clock regulatory elements control cyclic expression of Lunatic fringe during somitogenesis. *Dev Cell.* 3: 75-84.

Dale JK, M.M., Dequeant ML, Malapert P, McGrew M, Pourquie O. 2003. Periodic notch inhibition by lunatic fringe underlies the chick segmentation clock. *Nature* 421: 275-8.

Darnell DK, K.S., Stanislaw S, Konieczka JH, Yatskievych TA, Antin PB. 2006. MicroRNA expression during chick embryo development. *Dev Dyn.* 235: 3156-65.

Dubrulle J, M.M., Pourquié O. 2001. FGF signaling controls somite boundary position and regulates segmentation clock control of spatiotemporal Hox gene activation. *Cell* 106: 219-32.

Evrard YA, L.Y., Aulehla A, Gan L. and Johnson RL. 1998. Lunatic fringe is an essential mediator of somite segmentation and patterning. *Nature* 394: 377-381.

Forsberg H, C.F., Brown NA. 1998. Waves of mouse Lunatic fringe expression, in four-hour cycles at two-hour intervals, precede somite boundary formation. *Curr Biol.* 8: 1027-30.

Gomez C, O.E., Wunderlich J, Baumann D, Lewis J, Pourquié O. 2008. Control of segment number in vertebrate embryos. *Nature* 454: 335-9.

Gregory PA, B.C., Bert AG, Goodall GJ. 2008. MicroRNAs as regulators of epithelial-mesenchymal transition. *Cell Cycle* 7: 3112-8.

Hamilton, H.V.a.H. 1951. A Series of Normal Stages in the Development of the Chick. *Journal of Morphology* 88: 49-92.

Hicks C, J.S., diSibio G, Collazo A, Vogt TF, Weinmaster G. 2000. Fringe differentially modulates Jagged1 and Delta1 signalling through Notch1 and Notch2. *Nat Cell Biol.* 2: 515-20.

Hilgers V, P.O., Dubrulle J. 2005. In vivo analysis of mRNA stability using the Tet-Off system in the chicken embryo. *Dev Biol.* 284: 292-300.

Hirata H, B.Y., Kokubu H, Masamizu Y, Yamada S, Lewis J, Kageyama R. 2004. Instability of Hes7 protein is crucial for the somite segmentation clock. *Nat Genet.* 36: 750-4.

Hirsinger E, J.C., Dubrulle J, Pourquié O. 2000. Somite formation and patterning. *Int Rev Cytol.* 198: 1-65.

John B, E.A., Aravin A, Tuschl T, Sander C, Marks DS. 2004. Human MicroRNA targets. *PLoS Biol.* 2.

Korpal M, K.Y. 2008. The emerging role of miR-200 family of microRNAs in epithelial-mesenchymal transition and cancer metastasis. *RNA Biol.* 5: 115-9.

Lai EC, P.J. 1997. The Bearded box, a novel 3' UTR sequence motif, mediates negative post-transcriptional regulation of Bearded and Enhancer of split Complex gene. *Development* 124: 4847-56.

Leucht C, S.C., Wizenmann A, Klafke R, Folchert A, Bally-Cuif L. 2008. MicroRNA-9 directs late organizer activity of the midbrain-hindbrain boundary. *Nat Neurosci* 11: 641-8.

Levy AP, L.N., Goldberg MA. 1996. Hypoxia-inducible protein binding to vascular endothelial growth factor mRNA and its modulation by the von Hippel-Lindau protein. *J Biol Chem* 271: 25492-7.

Lewis BP, S.I., Jones-Rhoades MW, Bartel DP, Burge CB. 2003. Prediction of mammalian microRNA targets. *Cell* 115: 787-98.

Lewis, J. 2003. Autoinhibition with transcriptional delay: a simple mechanism for the zebrafish somitogenesis oscillator. *Curr Biol.* 13: 1398-408.

Lin Z, M.I., Wang K, Jiao J, Gao J, Li PF. 2009. miR-23a functions downstream of NFATc3 to regulate cardiac hypertrophy. *Proc Natl Acad Sci USA* 106: 12103-8.

McGrew MJ, D.J., Fraboulet S, Pourquié O. 1998. The lunatic fringe gene is a target of the molecular clock linked to somite segmentation in avian embryos. *Curr Biol.* 8: 979-82.

Monk, N. 2003. Oscillatory expression of Hes1, p53, and NF-kappaB driven by transcriptional time delays. *Curr Biol.* 13: 1409-13.

Morales AV, Y.Y., Ish-Horowicz D. 2002. Periodic Lunatic fringe expression is controlled during segmentation by a cyclic transcriptional enhancer responsive to notch signaling. *Dev Cell.* 3: 63-74.

Oginuma M, T.Y., Kitajima S, Kiso M, Kanno J, Kimura A, Saga Y. 2010. The oscillation of Notch activation, but not its boundary, is required for somite border formation and rostral-caudal patterning within a somite. *Development* 137: 1515-22.

Riddle RD, J.R., Laufer E, Tabin C. 1993. Sonic hedgehog mediates the polarizing activity of the ZPA. *Cell* 75: 1401-16.

Serth K, S.-G.K., Cordes R, Gossler A. 2003. Transcriptional oscillation of lunatic fringe is essential for somitogenesis. *Genes Dev.* 17: 912-25.

Sheedy FJ, P.-M.E., Hennessy EJ, Martin C, O'Leary JJ, Ruan Q, Johnson DS, Chen Y, O'Neill LA. 2010. Negative regulation of TLR4 via targeting of the proinflammatory tumor suppressor PDCD4 by the microRNA miR-21. *Nat Immunol.* 11: 141-7.

Shifley ET, V.K., Perez-Balaguer A, Franklin JD, Weinstein M, Cole SE. 2008. Oscillatory lunatic fringe activity is crucial for segmentation of the anterior but not posterior skeleton. *Development* 135: 899-908.

Shkumatava A, S.A., Sive H, Bartel DP. 2009. Coherent but overlapping expression of microRNAs and their targets during vertebrate development. *Genes Dev.* 23: 466-81.

Tadauchi T, M.K., Herskowitz I, Irie K. 2001. Post-transcriptional regulation through the HO 3'-UTR by Mpt5, a yeast homolog of Pumilio and FBF. *EMBO J* 20: 552-61.

Wightman B, H.I., Ruvkun G. 1993. Posttranscriptional regulation of the heterochronic gene lin-14 by lin-4 mediates temporal pattern formation in C. elegans. *Cell* 75: 855-62.

Xie X, L.J., Kulbokas EJ, Golub TR, Mootha V, Lindblad-Toh K, Lander ES, Kellis M. 2005. Systematic discovery of regulatory motifs in human promoters and 3' UTRs by comparison of several mammals. *Nature* 434: 338-45.

Xie ZR, Y.H., Liu WC, Hwang MJ. 2007. The role of microRNA in the delayed negative feedback regulation of gene expression. *Biochem Biophys Res Commun* 358: 722-6.

Zeiser S, L.H., Tiedemann H, Rubio-Aliaga I, Przemeck GK, de Angelis MH, Winkler G. 2006. Number of active transcription factor binding sites is essential for the Hes7 oscillator. *Theor Biol Med Model* 3.

Zeng L, C.A., Childs SJ. 2009. miR-145 directs intestinal maturation in zebrafish. *Proc Natl Acad Sci USA* 106: 17793-8.

Zhang Gridley. 1998. Defects in somite formation in Lunatic fringe deficient mice. *Nature* 394: 374-377.

Figure 1. A subset of microRNAs predicted to target the *Lfng* 3'UTR are enriched in the presomitic mesoderm (PSM). A. Comparison of the mouse, human, and chicken *Lfng* 3'UTR by mVista (Bray N 2003) demonstrate high levels of sequence conservation. Below, a schematic of the *Lfng* 3'UTR depicting conserved regions (with regions conserved mouse to human above the line and regions conserved mouse to chicken below the line). Predicted microRNA binding sites are also shown, with evolutionarily conserved binding sites in bold. B. RT-PCR of PSM and mature somite derived tissue from E9.5 mouse embryos using Taqman® microRNA specific primers. Results demonstrate upregulation of miR-125a-5p, miR-200b/c, and miR-429, downregulation of miR-125b and miR-204, and no change in miR-351and miR-211 expression levels in the PSM compared to mature somites. RT-PCR was conducted in triplicate on at least three biologically independent replicates. Results indicate mean +/- SD after normalizing expression levels of the somatic samples to 1. Significance is based on Student's T test. C, D. Whole-mount in-situ hybridization of mouse embryos using locked nucleic acid probes for mmu-miR-200b (C) and mmu-miR-125a-5p (D) demonstrates enrichment of these microRNAs in the posterior PSM.

Figure 2. The *Lfng* 3'UTR is an evolutionarily conserved target of miR-200b and miR-125a-5p. A. Luciferase assay demonstrating decreased luciferase activity in NIH3T3 cells co-transfected with pmiR-m*Lfng*-3'UTR and miR-200b. Point mutations in the miR-200b predicted binding site (MUT) abrogate this effect. B. Luciferase assay showing decreased luciferase activity in NIH3T3 cells co-transfected with pmiR-m*Lfng*-3'UTR and miR-125a-5p. Point mutations in the conserved (MUT3) or un-conserved (MUT1/MUT2) miR-125a-5p predicted binding sites abrogate this effect. C. Luciferase assay showing decreased luciferase activity in NIH3T3 cells co-transfected with pmiR-m*Lfng*-3'UTR and either scrambled miR or miR-200b/miR-125a-5p. Point mutations in all predicted binding sites for both miR-200b and miR-125a-5p (All MUT) abrogate this effect indicating the initial reduction observed in cells co-transfected with pmiR-m*Lfng*-3'UTR and scrambled miR was the result of endogenous miR activity. D. Luciferase assay showing decreased luciferase activity in cells co-transfected with pmiR-cLfng-3'UTR and miR-200b or miR-125a-5p. Point mutations in the predicted miR-200b (MUT1) or miR-125a-5p (MUT2) binding sites abrogate this effect. Abbreviations: m*Lfng*-3'UTR, mouse *Lfng* 3'UTR; c*Lfng*-3'UTR, chick *Lfng* 3'UTR. Results indicate Firefly luciferase activity normalized to Renilla luciferase activity $\pm$ SD. Each reporter plasmid was transfected at least three times and each sample was assayed in triplicate. Results were analyzed by ANOVA followed by Bonferroni post hoc.

Figure 3. Blocking interactions between endogenous miR-125a and *Lfng* perturbs segmentation. A. Target protector design: Predicted pairings of TP-*Lfng*^{ctrl}, TP-*Lfng*$^{miR\text{-}200b}$, and TP-*Lfng*$^{miR\text{-}125a}$ to the chick *Lfng* 3'UTR. B-E. Electroporation of TP-*Lfng*^{ctrl} has no effect on segmentation or differentiation as evidenced by normal Uncx4.1 (C) and MyoD (E) staining. F-I. Electroporation of TP-*Lfng*$^{miR\text{-}200b + miR\text{-}125a}$ disrupts positioning of somite boundaries and antero-posterior somite compartmentalization as evidenced by irregular Uncx4.1 staining (G) in the fluorescein positive somites (F). The onset of MyoD expression was visible (I) in fluorescein positive somites (H) indicative of proper differentiation. J-M. Electroporation of TP-*Lfng*$^{miR\text{-}125a}$ disrupts positioning/formation of somite boundaries and antero-posterior somite compartmentalization as evidenced by irregular Uncx4.1 staining (K) in the fluorescein positive somites compared to non-electroporated side (J). The onset of MyoD expression was visible in fluorescein positive somites (L-M). N-Q. Electroporation of TP-*Lfng*$^{miR\text{-}200b}$ has no effect on somite boundary formation or antero-posterior somite compartmentalization (O) or MyoD expression (Q).

Figure 4. Blocking interactions between endogenous miR-125a and *Lfng* perturbs cyclic expression of *Lfng* and *cHairy1*. A. In ovo electroporation of TP-*Lfng*^{ctrl} results in normal cyclic expression of endogenous *Lfng* (Compare with Supplementary Fig. 2a). B. Electroporation of TP-*Lfng*$^{miR\text{-}200b+miR\text{-}125a}$ abolishes cyclic expression of *Lfng*. Of 12 embryos electroporated with TP-*Lfng*$^{miR\text{-}200b+miR\text{-}125a}$, none exhibit expression of *Lfng* in the posterior PSM. C. Electroporation of TP-*Lfng*$^{miR\text{-}125a}$ abolishes cyclic expression of *Lfng*. Of 12 embryos electroporated with TP-*Lfng*$^{miR\text{-}125a}$, none exhibit expression of Lfng in the posterior PSM. D. Electroporation of TP-*Lfng*$^{miR\text{-}200b}$ has no effect on cyclic expression of *Lfng*. E. Electroporation of TP-*Lfng*^{ctrl} results in normal cyclic expression of endogenous *cHairy1* (Compare with Supplementary Fig. 2B). F Electroporation of TP-*Lfng*$^{miR\text{-}125a+200b}$ perturbs cyclic expression of cHairy1. Of 5 embryos, 2 exhibit an expression pattern similar to Phase I seen in control embryos, and 3 exhibit an expression pattern similar to that seen in Phase III of control embryos. Phase II was not observed. G. Electroporation of TP-*Lfng*$^{miR\text{-}125a}$ perturbs cyclic expression of *cHairy1*. Of 5 embryos electroporated with TP-*Lfng*$^{miR\text{-}125}$, all exhibit expression of *cHairy1* as a band in the rostral most part of the PSM and expression in the tail bud extending into the middle of the PSM, similar to that observed in Phase I of control embryos. Phases I and II were not observed. Abbreviations: Fl, fluorescein.

Figure 1

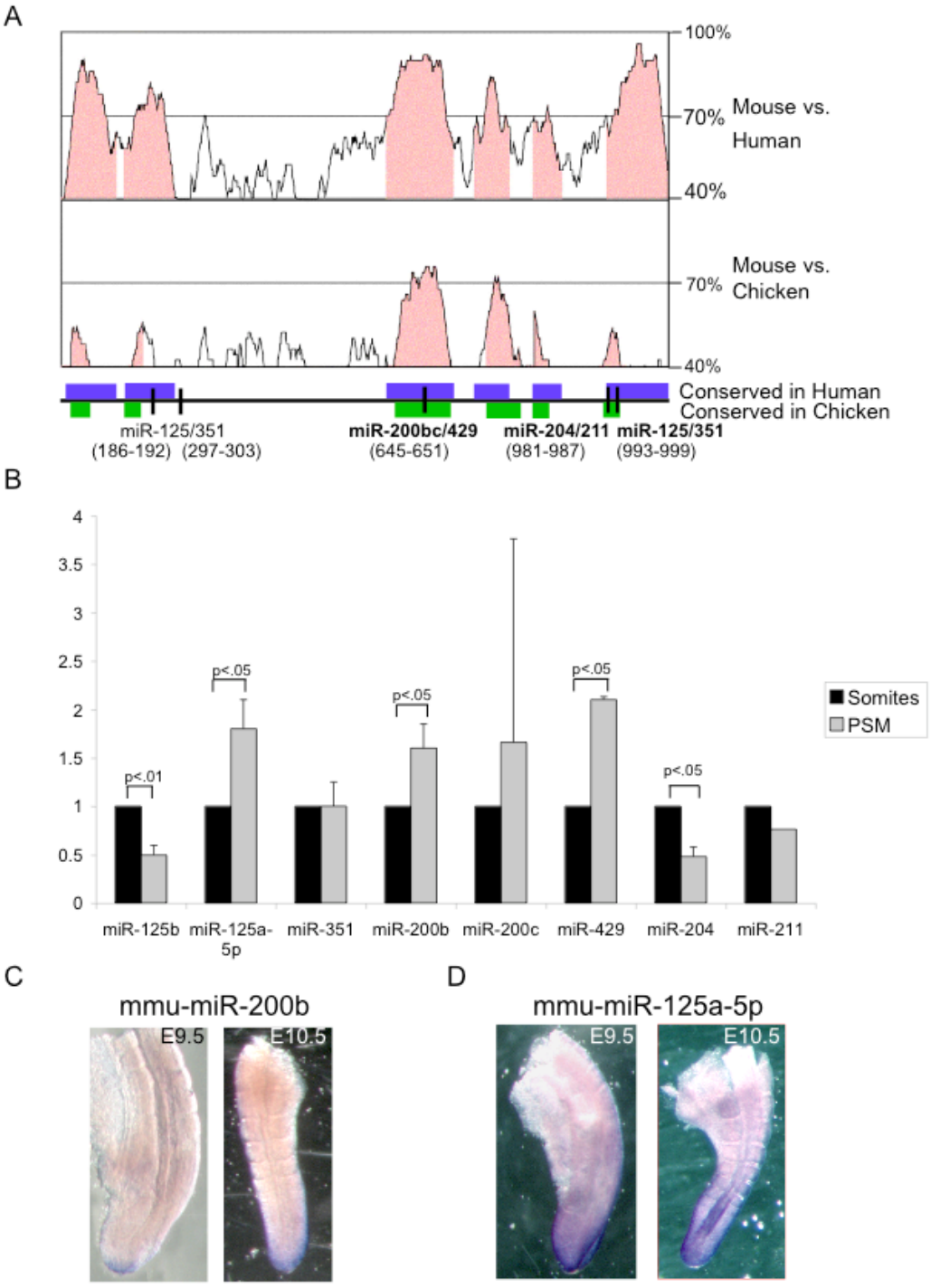
A
100%
70%
Mouse vs. Human
40%
70%
Mouse vs. Chicken
40%
Conserved in Human
Conserved in Chicken
miR-125/351 (186-192) (297-303)
miR-200bc/429 (645-651)
miR-204/211 (981-987)
miR-125/351 (993-999)
B
4
3.5
3
2.5
2
1.5
1
0.5
0
p<.01
p<.05
p<.05
p<.05
p<.05
Somites
PSM
miR-125b
miR-125a-5p
miR-351
miR-200b
miR-200c
miR-429
miR-204
miR-211
C
mmu-miR-200b
E9.5
E10.5
D
mmu-miR-125a-5p
E9.5
E10.5

Figure 2

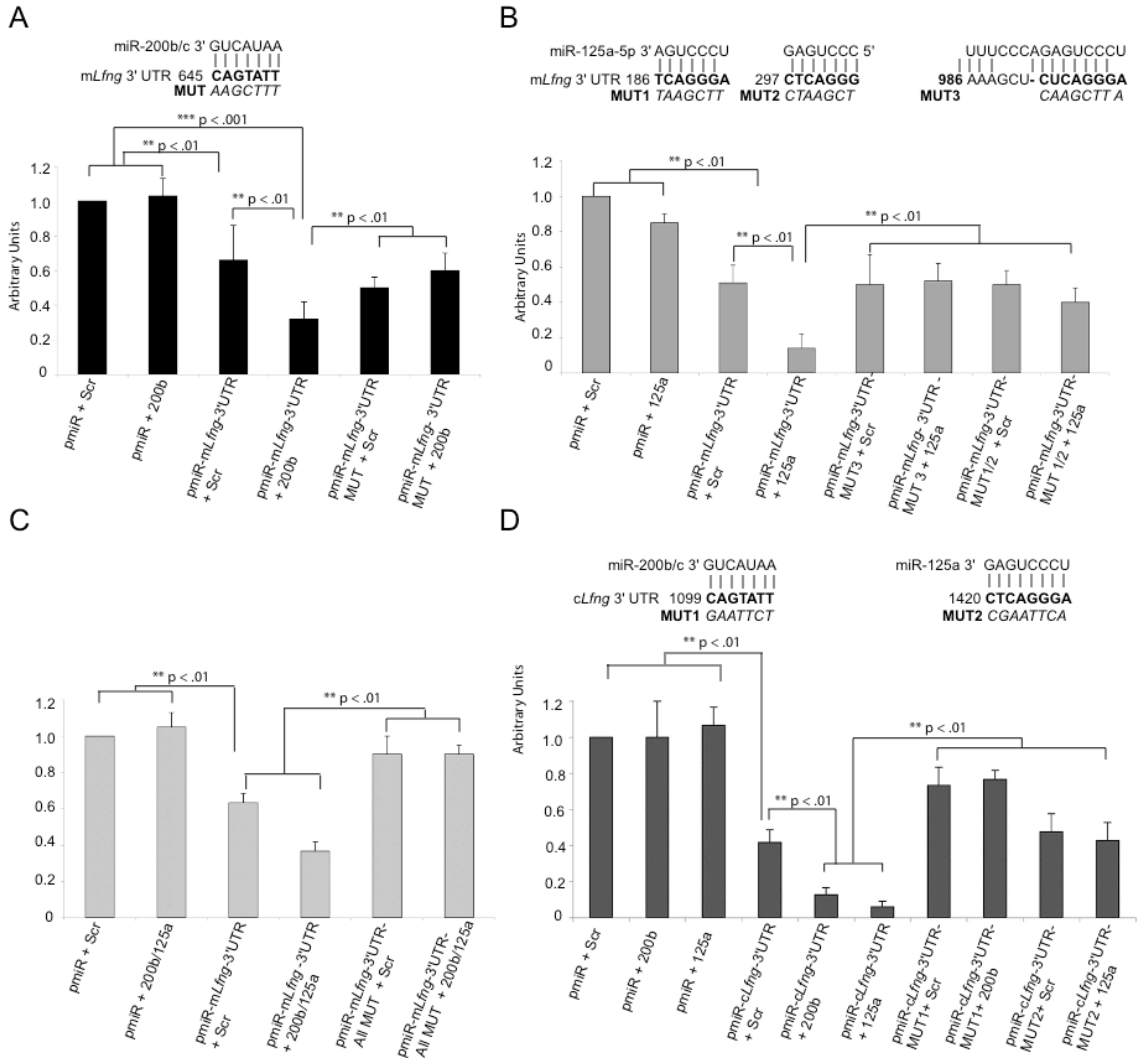
A
miR-200b/c 3' GUCAUAA
mLfng 3' UTR 645 CAGTATT
MUT AAGCTTT
*** p < .001
** p < .01
** p < .01
** p < .01
Arbitrary Units
pmiR + Scr
pmiR + 200b
pmiR-mLfng-3'UTR + Scr
pmiR-mLfng-3'UTR + 200b
pmiR-mLfng-3'UTR MUT + Scr
pmiR-mLfng- 3'UTR MUT + 200b
B
miR-125a-5p 3' AGUCCCU
GAGUCCC 5'
mLfng 3' UTR 186 TCAGGGA
297 CTCAGGG
MUT1 TAAGCTT
MUT2 CTAAGCT
UUUCCCAGAGUCCCU
986 AAAGCU- CUCAGGGA
MUT3 CAAGCTT A
** p < .01
** p < .01
** p < .01
Arbitrary Units
pmiR + Scr
pmiR + 125a
pmiR-mLfng-3'UTR + Scr
pmiR-mLfng-3'UTR + 125a
pmiR-mLfng-3'UTR-MUT3 + Scr
pmiR-mLfng- 3'UTR-MUT 3 + 125a
pmiR-mLfng-3'UTR-MUT1/2 + Scr
pmiR-mLfng-3'UTR-MUT 1/2 + 125a
C
** p < .01
** p < .01
pmiR + Scr
pmiR + 200b/125a
pmiR-mLfng-3'UTR + Scr
pmiR-mLfng -3'UTR + 200b/125a
pmiR-mLfng-3'UTR-All MUT + Scr
pmiR-mLfng-3'UTR-All MUT + 200b/125a
D
miR-200b/c 3' GUCAUAA
miR-125a 3' GAGUCCCU
cLfng 3' UTR 1099 CAGTATT
1420 CTCAGGGA
MUT1 GAATTCT
MUT2 CGAATTCA
** p < .01
** p < .01
** p < .01
Arbitrary Units
pmiR + Scr
pmiR + 200b
pmiR + 125a
pmiR-cLfng-3'UTR + Scr
pmiR-cLfng-3'UTR + 200b
pmiR-cLfng-3'UTR + 125a
pmiR-cLfng-3'UTR-MUT1+ Scr
pmiR-cLfng-3'UTR-MUT1+ 200b
pmiR-cLfng-3'UTR-MUT2+ Scr
pmiR-cLfng-3'UTR-MUT2 + 125a

Figure 3

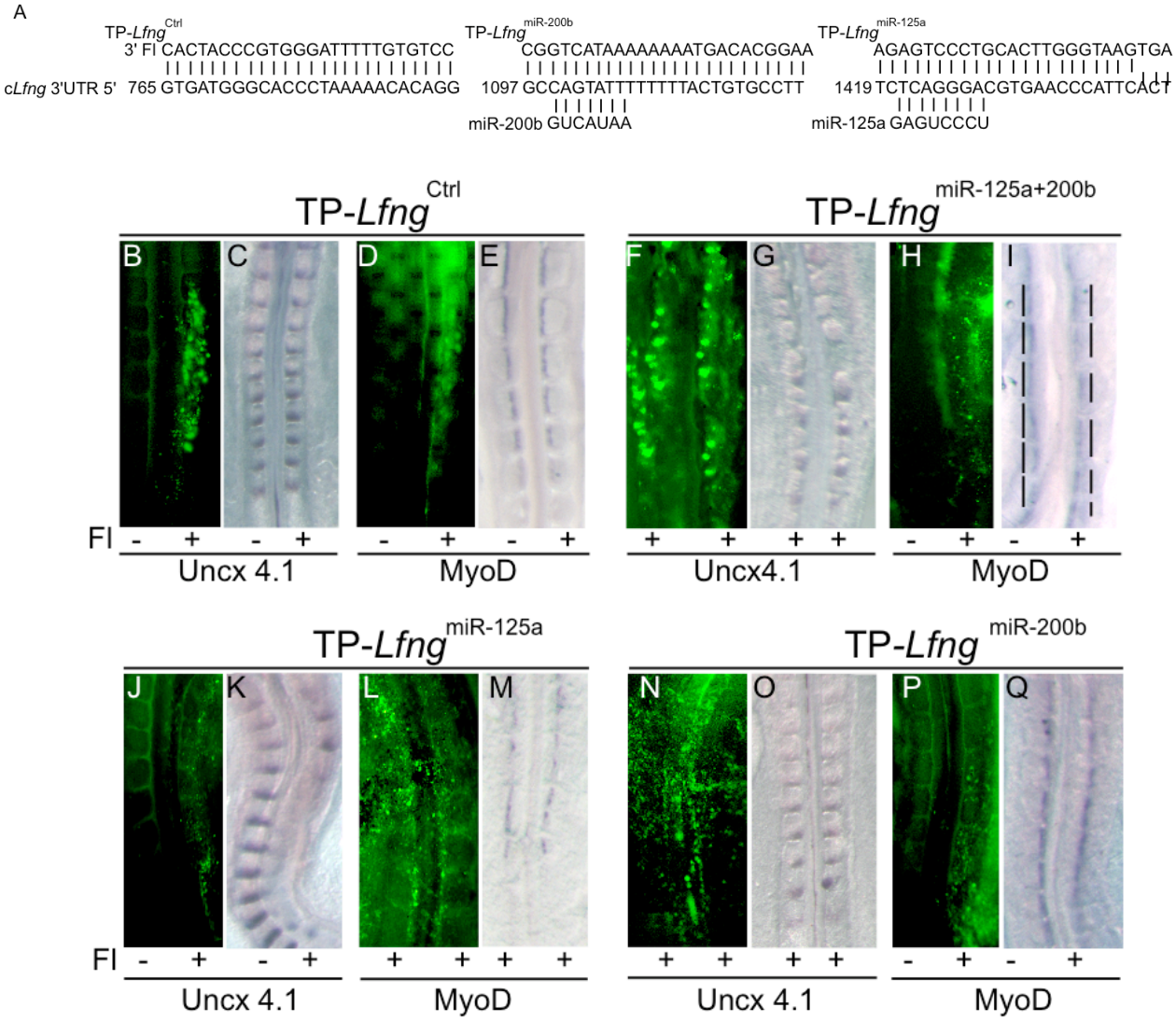
A
TP-Lfng Ctrl
3' Fl CACTACCCGTGGGATTTTTGTGTCC
cLfng 3'UTR 5' 765 GTGATGGGCACCCTAAAAACACAGG
TP-Lfng miR-200b
CGGTCATAAAAAAAATGACACGGAA
1097 GCCAGTATTTTTTTTACTGTGCCTT
miR-200b GUCAUAA
TP-Lfng miR-125a
AGAGTCCCTGCACTTGGGTAAGTGA
1419 TCTCAGGGACGTGAACCCATTCACT
miR-125a GAGUCCCU
TP-Lfng Ctrl
TP-Lfng miR-125a+200b
TP-Lfng miR-125a
TP-Lfng miR-200b
B C D E F G H I J K L M N O P Q
Fl
Uncx 4.1
MyoD
Uncx4.1
MyoD
Uncx 4.1
MyoD
Uncx 4.1
MyoD

Figure 4

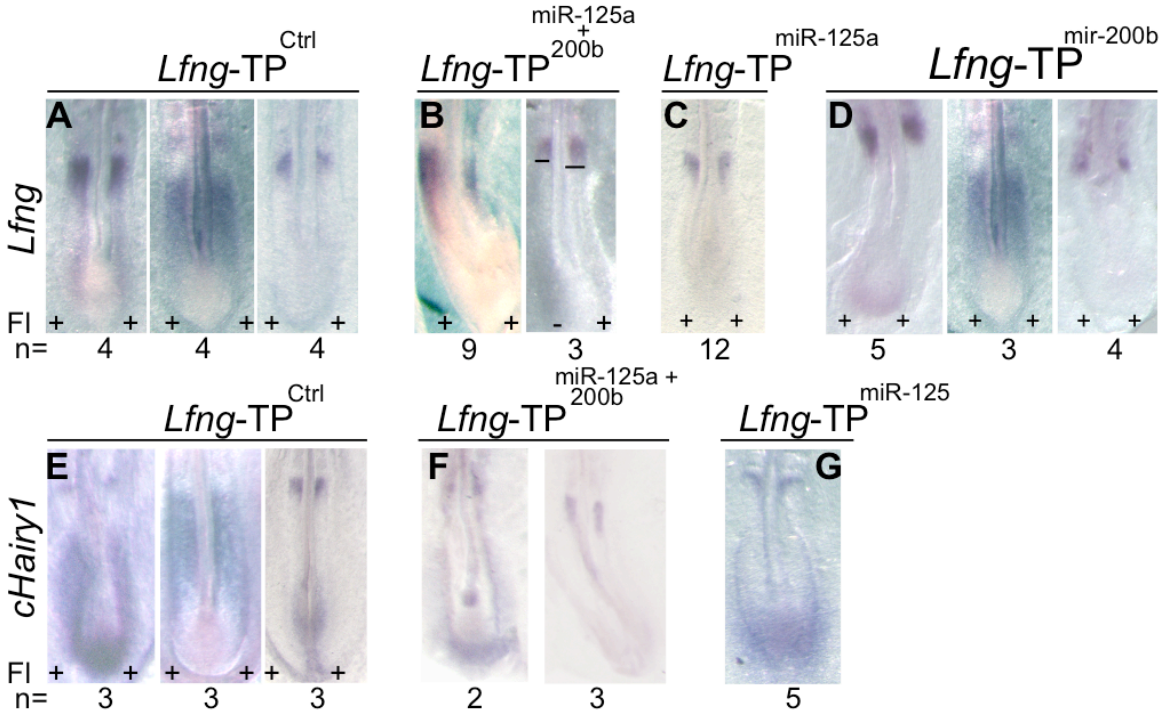
Lfng-TP Ctrl
Lfng-TP miR-125a + 200b
Lfng-TP miR-125a
Lfng-TP mir-200b
A
B
C
D
Lfng
Fl + + + + + +
n= 4 4 4
+ + - + + +
9 3 12 5 3 4
Lfng-TP Ctrl
Lfng-TP miR-125a + 200b
Lfng-TP miR-125
E
F
G
cHairy1
Fl + + + + + +
n= 3 3 3
2 3 5

Supplementary Figure 1. Target Protectors Effectively Inhibit microRNA interactions with the *Lfng* 3'UTR without affecting protein synthesis in cell culture. An equivalent reduction in luciferase activity is observed when NIH 3T3 cells are co-transfected with miR-*Lfng*-3'UTR + miR-200b or miR-*Lfng*-3'UTR + miR-200b + TP^{Ctrl} indicating the TP^{Ctrl} has no effect on binding of miR-200b to the *Lfng* 3'UTR or on normal protein synthesis. This reduction is lost upon co-transfection of miR-*Lfng*-3'UTR + miR-200b + $TP^{miR\text{-}200b}$, indicating $TP^{miR\text{-}200b}$ effectively blocks interactions between miR-200b and the Lfng 3'UTR. Similarly, an equivalent reduction in luciferase activity is observed when NIH 3T3 cells are co-transfected with miR-*Lfng*-3'UTR + miR-125a or miR-*Lfng*-3'UTR + miR-125a + TP^{Ctrl} indicating the TP^{Ctrl} has no effect on binding of miR-125a to the *Lfng* 3'UTR or on normal protein synthesis. This reduction is lost upon co-transfection of miR-*Lfng*-3'UTR + miR-125a + $TP^{miR\text{-}125a}$, indicating $TP^{miR\text{-}125a}$ effectively blocks interactions between miR-125a and the *Lfng* 3'UTR. Results indicate Firefly luciferase activity normalized to Renilla luciferase activity +/- SD. Each experiment was performed at least times in triplicate. Results were analyzed by ANOVA followed by Bonferonni post hoc.

Supplementary Figure 2. Cyclic expression of *Lfng* and *cHairy1* in non-electroporated chick embryos. A. Embryos of stages 9-10 HH exhibit cyclic expression of *Lfng*. B. Embryos of stages 9-10 HH exhibit cyclic expression of *cHairy*. Embryos were fixed at room temperature for 4 hours and processed for whole mount in-situ hybridization using a *Lfng or cHairy1* coding probe as described in Materials and Methods.

Supplementary Figure 1

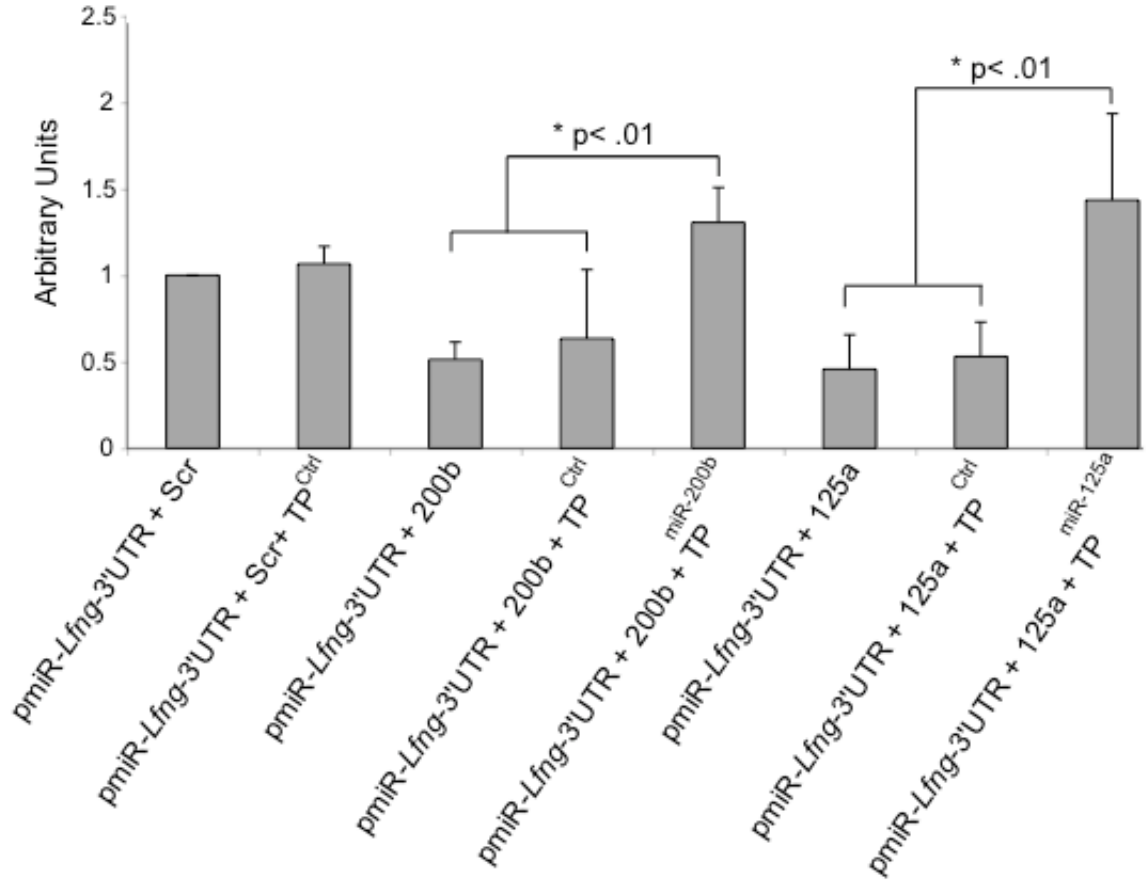

Supplementary Figure 2